Journal of Molecular Graphics and Modelling 41 (2013) 61–67

Contents lists available at SciVerse ScienceDirect

Journal of Molecular Graphics and Modelling

journal homepage: www.elsevier.com/locate/JMGM

3D-QSAR studies of azaoxoisoaporphine, oxoaporphine, and oxoisoaporphine derivatives as anti-AChE and anti-AD agents by the CoMFA method

Yan-Ping Li, Xiang Weng, Fang-Xian Ning, Jie-Bin Ou, Jin-Qiang Hou, Hai-Bin Luo*, Ding Li, Zhi-Shu Huang, Shi-Liang Huang**, Lian-Quan Gu

School of Pharmaceutical Sciences, Sun Yat-sen University, Guangzhou 510006, People's Republic of China

ARTICLE INFO

Article history:
Accepted 7 February 2013
Available online 16 February 2013

Keywords:
Azaoxoisoaporphine derivatives
Alzheimer's disease
AChE inhibitors
Aβ aggregation
3D-QASR
CoMFA

ABSTRACT

In the present study, a series of novel azaoxoisoaporphine derivatives were reported and their inhibitory activities toward acetylcholinesterase (AChE), butyrylcholinesterase (BuChE), and Aβ aggregation were evaluated. The new compounds remained high inhibitory potency on Aβ aggregation, with inhibitory activity from 29.42% to 89.63% at a concentration of 10 μM, but had no action on AChE or BuChE, which was very different from our previously reported oxoaporphine and oxoisoaporphine derivatives. By 3D-QSAR studies, we constructed a reliable CoMFA model ($q^2 = 0.856$ and $r^2 = 0.986$) based on the inhibitory activities toward AChE and discovered key information on structure and anti-AChE activities among the azaoxoisoaporphine, oxoaporphine, and oxoisoaporphine derivatives. The model was further confirmed by the test-set validation ($q^2 = 0.873$, $r^2 = 0.937$, and slope $k = 0.902$) and Y-randomization examination. The statistically significant and physically meaningful 3D-QSAR/CoMFA model provided better insight into understanding the inhibitory behaviors of those chemicals, which may provide useful information for the rational molecular design of azaoxoisoaporphine derivatives anti-AChE and anti-AD agents.

1. Introduction

As the population of elder people is increasing rapidly, Alzheimer's disease (AD) has become a serious social problem all around the world. Nowadays, about 18 million elder people are suffering from AD and this number is increasing year by year [1]. AD is a neurodegenerative disease. Though several factors are discovered to relate closely with its development, such as acetylcholine (ACh) dysfunction, amyloid β protein (Aβ) aggregation, tau protein aggregation, and oxidative stress, there is still no effective drugs which could prevent AD progress. In view of these factors, small molecules have been vastly discovered, but so far only acetylcholinesterase (AChE) inhibitors and a N-methyl D-aspartate antagonist memantine were approved for clinical uses [2].

Compounds which could interact with two or more targets of AD are of great interest for the AD therapy in recent years. In our laboratory, several series of oxoaporphine and oxoisoaporphine derivatives have been previously reported to be potential anti-AD agents, which exhibited inhibitory activities on AChE, butyrylcholinesterase (BuChE), and Aβ aggregation [3–5]. SAR (structure–activity relationship) studies demonstrated that oxoisoaporphine derivatives exhibited better AChE inhibitory activities than oxoaporphine derivatives generally, and their inhibitory activities were closely related to terminal groups and substituted positions. Compounds with quaternary nitrogen were found to have higher inhibitory activities for both AChE and Aβ aggregation. Besides, derivatives with higher selectivity on AChE over butyrylcholinesterase (BuChE) also exhibited high inhibitory potency on Aβ aggregation.

Recently, several groups have paid attention to the modification and synthesis of oxoaporphine and oxoisoaporphine derivatives [6–9], and our group had reported four series of novel oxoaporphine and oxoisoaporphine derivatives [3–5]. In the present study, firstly a series of azaoxoisoaporphine derivatives, were synthesized (**7a–7g**) and subjected to inhibitory tests toward AChE, BuChE, Aβ aggregation and MTT assay. It was found that though these compounds remained high inhibitory potency on Aβ aggregation, they totally lost ChE inhibitory activity. The findings are interesting because oxoaporphine and oxoisoaporphine derivatives were good ChE inhibitors previously reported by us. Secondly, 3D-QSAR (three-dimensional quantitative structure–activity relationship) analyses of these azaoxoisoaporphine compounds plus our previously reported oxoaporphine and oxoisoaporphine derivatives [3–5] by using the CoMFA (comparative molecular field analysis) approach [10,11] were performed. The derived 3D-QSAR model resulted in a robust structure–activity correlation ($q^2 = 0.856$ and

* Corresponding author. Tel.: +86 20 39943031.
** Corresponding author. Tel.: +86 20 39943052; fax: +86 20 39943056.
E-mail addresses: luohb77@mail.sysu.edu.cn (H.-B. Luo), lsshsl@mail.sysu.edu.cn (S.-L. Huang).

1093-3263/$ – see front matter
http://dx.doi.org/10.1016/j.jmgm.2013.02.003

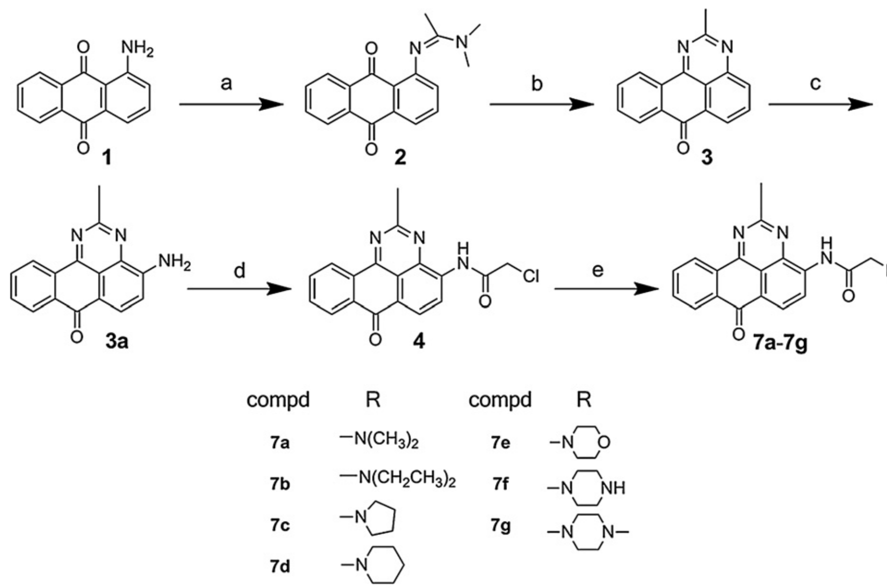

Scheme 1. Synthesis of compounds **7a**–**7g**. Reagents and conditions: (a) $POCl_3$, $MeCONMe_2$, 50 °C, 6 h, 94%; (b) NH_4OAc, EtOH, reflux 2 h, 90%; (c) $NH_2OH(HCl)$, NaOH, DEG, 100 °C, 15 min, 73%; (d) $ClCOCH_2Cl$, K_2CO_3, $CHCl_3$, reflux, 6 h, 89%; (e) amine, K_2CO_3, KI, DMF, 50 °C.

r^2 = 0.986) based on their AChE inhibitory activities, which may provide useful information for the rational molecular design of azaoxoisoaporphine derivatives as anti-AChE and anti-AD agents.

2. Materials and methods

2.1. Synthesis and bioassay of compounds 7a–7g

The synthetic path was shown in Scheme 1. Started with 1-amino anthraquinone, compound **3** was obtained by two step reactions as previously reported by Bu et al. and our team [12,13]. Then amino group was introduced at 4-position to get intermediate **3a** and linker was added by acylation of amine to get intermediate **4**. Seven final products were obtained by reacting **4** with different amines. They were characterized by using ^{1}H NMR, ^{13}C NMR, and HRMS which could be found in Supporting Information. Their structures and evaluation results were summarized in Tables 1 and 2. All biological methods were also presented in Supporting Information.

2.2. Data set for statistical analyses

The AChE experimental data of 41 oxoaporphine and oxoisoaporphine derivatives have been published previously [3–5], which were used in the present statistical analyses. All biological data were expressed as pIC_{50} ($-\log IC_{50}$). The pIC_{50} values had a broad span of 5 log units, suggesting a diverse data set for our QSAR study. A training set of 40 molecules (Table 1) was used to generate QSAR models. The molecules in training set were selected according to the criteria that they contained both structural and biological activity information. The remaining 8 molecules (Table 2) constituted the test set. For compounds **7a**–**7g**, 100 μM were taken as their IC_{50} values in order to carry out the modeling study. In fact, 1000 μM was also used as their IC_{50} values to construct CoMFA models. It was found that two derived CoMFA models had no significant difference (data shown below). Thus, only 100 μM was used for the new compounds.

2.3. Molecular alignment

All initial models were built by using the Tripos Sybyl 7.3.5 software. The predictive accuracy of a CoMFA model and the reliability of contour maps depended strongly on structural alignment of molecules studied. In this QSAR study, molecular alignment was obtained by the SYBYL routine database alignment protocol. The most active compound (**27**) was used as template. Energy minimizations were performed by using Tripos force field adopting Gasteriger–Hückel partial-atomic charges [14,15], with the Powell conjugate-gradient minimization algorithm and a convergence criterion of 0.05 kcal/(mol Å). The aligned compounds were displayed in Fig. 1.

2.4. 3D-QSAR model generation

Steric and electrostatic potential fields for CoMFA were calculated at each lattice intersection of a regularly spaced grid box. Lattice spacing was set to a value of 2.0 Å in all *X*, *Y* and *Z* directions. An sp^3 carbon atom with a charge of +1.0 served as the probe atom to calculate steric and electrostatic fields. The cut-off was set to 30 kcal/mol. Cross-validated regression coefficient (q^2) values were calculated by using partial the least-squares (PLS) methodology [16–18]. Leave-one-out (LOO) cross-validation was used to obtain optimum number of components (ONC) [19]. The final non-cross-validated model was developed with ONC to yield conventional regression coefficient (r^2) value, *F* value, and *S* value (standard error of estimate).

3. Results and discussion

3.1. AChE, BuChE, Aβ aggregation inhibition and MTT results of 7a–7g

These results were summarized in Table 3. Compared with our previous oxoisoaporphine derivatives, compounds bearing this azaoxoisoaporphine ring did not show any inhibitory effect on either AChE or BuChE even at 100 μM. However, they still had potential inhibitory potency on Aβ aggregation, with inhibitory activity from 29.42% to 89.63% at concentration 10 μM, and **7a**–**7e** exhibited higher inhibition than curcumin at this concentration. MTT assay showed that except **7f** (IC_{50} = 8.26 μM) the rest of them had IC_{50} values more than 50 μM, which implied that they were not toxic to cells even at high concentrations. From these data, it could be concluded that structural modifications

Table 1
Azaoxoisoaporphine, oxoaporphine, and oxoisoaporphine derivatives in the training set and their experimental and predicted AChE inhibitory activities (pIC_{50} values).[a]

Cpd.		R	*n*	Experimental pIC_{50}	Predicted pIC_{50}	Differences
1	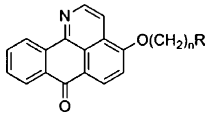	$-N(CH_2CH_3)_2$	2	6.697	6.868	0.164
2			3	7.465	7.127	0.375
3		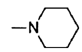	3	7.658	7.239	0.570
4		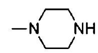	2	6.365	6.514	−0.050
5			3	6.393	6.808	−0.558
6	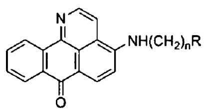	$-N(CH_3)_2$	3	6.400	6.638	0.062
7	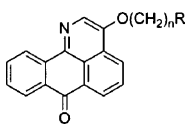	$-N(CH_3)_2$	2	5.807	6.080	−0.266
8		$-N(CH_2CH_3)_2$	2	6.155	6.262	0.175
9		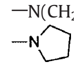	2	6.327	6.292	0.225
10		$-\overset{+}{N}(CH_3)_3$	2	6.030	6.124	−0.581
11		$-\overset{+}{N}(CH_3)(CH_2CH_3)_2$	2	6.588	6.540	−0.044
12		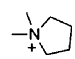	2	6.839	6.652	0.198
13	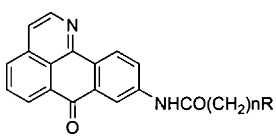	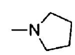	1	8.209	8.008	0.419
14			2	8.607	8.260	0.432
15		$-N(CH_3)_2$	1	7.016	7.276	−0.368
16			2	7.470	7.786	−0.419
17			3	7.516	7.561	−0.195
18		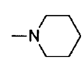	2	8.730	8.507	0.216
19		$-N(CH_2CH_3)_2$	2	7.936	7.946	−0.110
20		$-NH(CH_2)_2N(CH_3)_2$	2	6.921	6.811	−0.160
21		$-NH(CH_2)_2OH$	2	7.259	7.405	−0.060
22		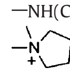	1	8.967	8.982	0.425
23			2	8.600	8.642	0.185
24		$-\overset{+}{N}(CH_3)_3$	1	7.825	7.769	−0.210
25			2	8.318	8.138	−0.241
26			3	8.320	8.515	−0.197
27		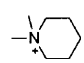	2	9.319	9.352	0.022
28	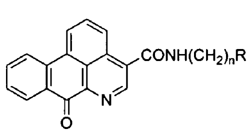	$-OH$	2	4.745	4.610	0.144
29		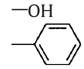	2	4.451	4.397	0.097
30		$-OH$	3	4.915	4.691	0.422
31		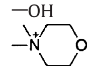	2	5.907	5.750	−0.133
32		$-\overset{+}{N}(CH_3)(CH_2CH_3)_2$	2	5.767	5.831	−0.131
33		$-\overset{+}{N}(CH_3)_3$	3	5.500	5.604	−0.375
34		$-\overset{+}{N}(CH_3)(CH_2CH_3)_2$	3	6.187	6.230	0.223
35 (**7a**)	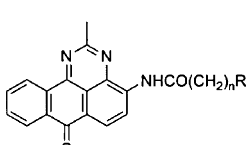	$-N(CH_3)_2$	1	4.000	4.232	−0.244
36 (**7b**)		$-N(CH_2CH_3)_2$	1	4.000	3.996	−0.035
37 (**7c**)		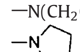	1	4.000	3.926	−0.039
38 (**7e**)		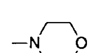	1	4.000	3.993	−0.028
39 (**7f**)		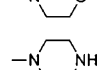	1	4.000	3.930	0.029
40 (**7g**)		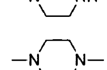	1	4.000	3.914	0.062

[a] Oxoaporphine and oxoisoaporphine derivatives (**1**–**34**) came from our previous studies [3–5]. $pIC_{50} = -\log IC_{50}$.

from oxoisoaporphines to azaoxoisoaporphines affected AChE and BuChE inhibitory activities dramatically among these derivatives, but with less effect on their abilities on Aβ aggregation.

According to our previous study [3–5], oxoisoaporphine derivatives had excellent inhibition on AChE, which ranged from nM to μM scale. It is strange that they totally lose this ability with little change on the mother ring. In order to get detail information

Table 2
Azaoxoisoaporphine, oxoaporphine, and oxoisoaporphine derivatives in the test set and their experimental and predicted AChE inhibitory activities (pIC_{50} values).[a]

Compd		R	*n*	Observed pIC_{50}	Predicted pIC_{50} (CoMFA)	Differences
41	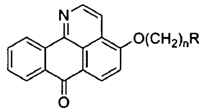	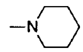	2	7.056	6.200	0.856
42	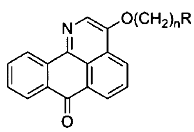	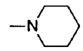	2	6.426	6.216	0.210
43		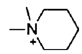	2	7.022	6.618	0.404
44	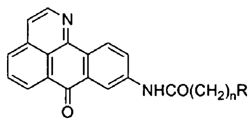	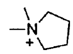	2	8.975	9.060	−0.085
45		$-\overset{+}{N}(CH_3)(CH_2CH_3)_2$	2	8.582	8.517	0.065
46 (**7d**)	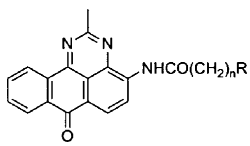	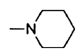	1	4.000	4.506	−0.506
47	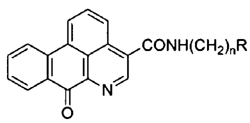	$-\overset{+}{N}(CH_3)_3$	2	5.479	5.688	−0.209
48		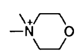	3	5.979	5.767	0.212

[a] Oxoaporphine and oxoisoaporphine derivatives (**41**–**45**, **47**–**48**) came from our previous studies [3–5]. $pIC_{50} = -\log IC_{50}$.

on SAR between these compounds and AChE, 3D-QSAR analyses were performed on both the new compounds and our previously reported oxoaporphine and oxoisoaporphine derivatives [3–5] by the CoMFA approach.

3.2. 3D-QSAR analysis by CoMFA and validations

The predictive power and robustness of the CoMFA models was evaluated by the cross-validated correlation coefficient (q^2) obtained by the LOO cross-validation procedures. Results of the CoMFA analysis based on the AChE inhibitory activities were shown in Table 4. For the CoMFA study, the cross-validated regression coefficient q^2 by LOO analysis was 0.856 at ONC 7. Non-cross-validated PLS analysis gave a conventional regression coefficient r^2 value of 0.986, F value of 316.535, and S value of 0.207, respectively. Steric field descriptor explained 58.3% of the variance, whereas electrostatic field counterpart explained 41.7% of the variance. The steric contribution to the model was higher than the electrostatic counterpart, which implied that inhibitory activities of compounds greatly depended on molecular shape, size and charge.

Predicted pIC_{50}, experimental pIC_{50}, and their differences for the training set molecules were listed in Table 3. A linear correlation between the predicted and experimental pIC_{50} values was shown in Fig. 2, which demonstrated that the predicted pIC_{50} values were in good agreement with the experimental pIC_{50} values.

When 1000 μM was used as the IC_{50} values of **7a**–**7g**, another CoMFA model achieved q^2 of 0.903, r^2 of 0.990, F value of 476.454, and S value of 0.197, respectively, which was quite similar to those by using 100 μM as the IC_{50} values of **7a**–**7g**. Thus we confirmed that our derived model was reasonable and could be applied to further discussion.

CoMFA analyses based on the BuChE inhibitory activities were also performed. As a result, a moderate model was generated at ONC 6 with r^2 of 0.822, q^2 of 0.760, S value of 0.373, and F value of 58.729. For an acceptable 3D-QSAR model, the resulting r^2 and q^2 values should be more than 0.9 and 0.5, respectively. Thus, only the

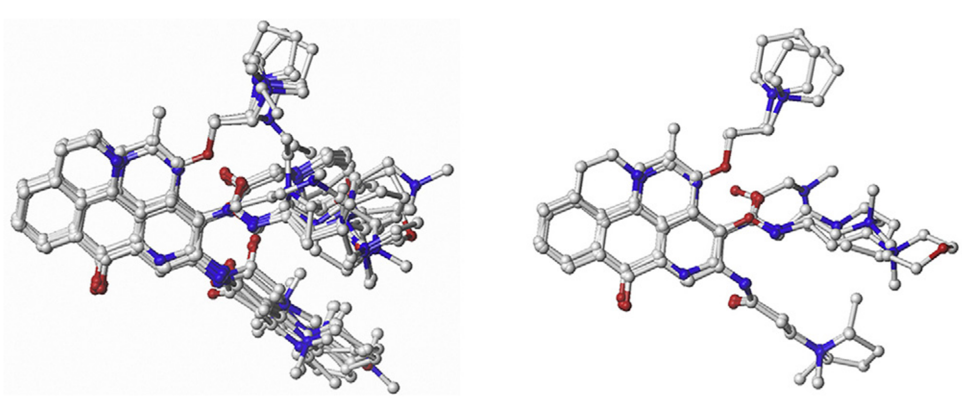

Fig. 1. Alignment of chemicals in the training set (LHS) and the test set (RHS).

Table 3
Structures of azaoxoisoaporphine derivatives and their affinities on AChE, BuChE, Aβ aggregation, and cell toxicity, respectively.

Compd	IC_{50} (μM)		Aβ inhibition (%)[c]	IC_{50} (μM)[d]
	AChE[a]	BuChE[b]		
7a	>100	>100	58.47	>100
7b	>100	>100	58.03	>100
7c	>100	>100	84.73	>100
7d	>100	>100	36.39	>100
7e	>100	>100	46.54	>100
7f	>100	>100	89.63	8.26
7g	>100	>100	29.42	52.57
Tacrine	0.278 ± 0.021	0.146 ± 0.032	–	–
Curcumin	–	–	32.76	–

[a] Inhibitor concentration (mean ± SEM of three experiments) required for 50% inactivation of AChE.
[b] Inhibitor concentration (mean ± SEM of three experiments) required for 50% inactivation of BuChE.
[c] Inhibition of self-induced Aβ (1–42) aggregation with the tested compounds at a concentration of 10 μM.
[d] Results obtained with MTT for SH-SY5Y cell line.

Table 4
Statistical results of the CoMFA model.

Model	q^2	r^2	S	E	*S* value	*F* value	ONC
CoMFA	0.856	0.986	58.3%	41.7%	0.207	316.535	7

Abbreviations: S, steric; E, electrostatic.

CoMFA model based on the AChE inhibitory activities was subjected to further discussion.

In order to evaluate the possibility of chance correlation in the above 3D-QSAR model, the compounds in the training set was performed by Y-randomization tests [20–23]. The Y-randomization test is generally used to ensure the robustness of a 3D-QSAR model. For this technique, the dependent variable vector (activity) is randomly shuffled and a new QSAR model is developed using the original independent variable matrix. If new QSAR models generate lower q^2 values for several examinations, then the resulting QSAR model is not derived by chance correlation and is validated to be robust. In the present study, none of q^2 values (Table 5) for fifty Y-randomization tests was more than 0.3 based on the CoMFA model, which further validated that the above CoMFA model was very robust.

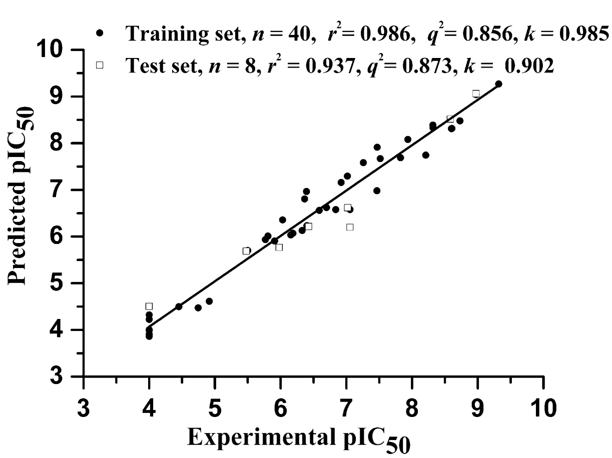

Fig. 2. Linear relationships of experimental and predicted AChE pIC_{50} values for compounds in the training set (circle) and the test set (pane) based on the derived CoMFA model.

Table 5
The average of the cross-validated regression coefficient q^2 values for the Y-randomization tests.

No.	q^2	No.	q^2
1	0.101	26	0.102
2	−0.213	27	0.123
3	0.123	28	−0.231
4	0.153	29	0.241
5	0.081	30	0.012
6	−0.242	31	0.125
7	0.031	32	0.215
8	0.073	33	−0.220
9	0.167	34	−0.123
10	−0.213	35	0.199
11	−0.251	36	0.010
12	−0.153	37	−0.102
13	0.143	38	0.210
14	0.267	39	0.156
15	0.059	40	0.264
16	−0.101	41	0.025
17	0.121	42	0.197
18	0.014	43	−0.186
19	0.057	44	−0.412
20	0.123	45	0.123
21	0.123	46	0.261
22	−0.286	47	−0.142
23	−0.356	48	0.213
24	−0.215	49	0.267
25	0.123	50	−0.451

3.3. External test-set validation of the CoMFA model

To further evaluate the predictive ability and robustness of the above 3D-QSAR model, external test-set validation of the CoMFA model was carried out by using a test set containing 8 compounds. For an acceptable 3D-QSAR model, the statistically recommendatory criteria are $r^2 \geq 0.6$, $q^2 \geq 0.5$, and $1.15 \geq$ slope $k \geq 0.85$ for the test set, respectively. Predicted pIC_{50}, experimental pIC_{50}, and their differences for the test set compounds were listed in Table 2, and the resulting q^2, r^2, and slope k values were 0.937, 0.873, and 0.902, respectively, suggested the CoMFA model derived from the training set compounds can satisfied the statistical criteria via the external test-set validation. The statistically significant correlation between experimental and predicted pIC_{50} values was shown in Fig. 2, which suggested that the derived 3D-QSAR model was robust and exhibited reliable predictive abilities, thus could also be used to estimate the inhibitory activities of newly synthesized analogs.

3.4. Contour analysis

Based on the 3D-QSAR/CoMFA model, contour maps were generated in order to better understand how structural modifications affected their activities.

Fig. 3A displayed the steric contour map of the CoMFA model based on compounds in the training set. Green region represented sterically favorable properties, whereas yellow region represented sterically unfavorable properties. A large green region was found around 9-substituted position indicating that bulk groups in this region were favorable for inhibitory activity. This may be the reason why compounds with side chains at this position were generally more potent than other compounds. For example, compounds **17**–**27** were generally more potent than compounds with side chains in other positions.

On the other hand, a large yellow contour was found near A ring, suggesting that a bulk group in this region would decrease inhibitory activity. This result is consistent with the fact that **7a**–**7g** with a methyl group in this position had no inhibitory effect on enzymatic activity, indicating bulky substitution at this place is not favorable.

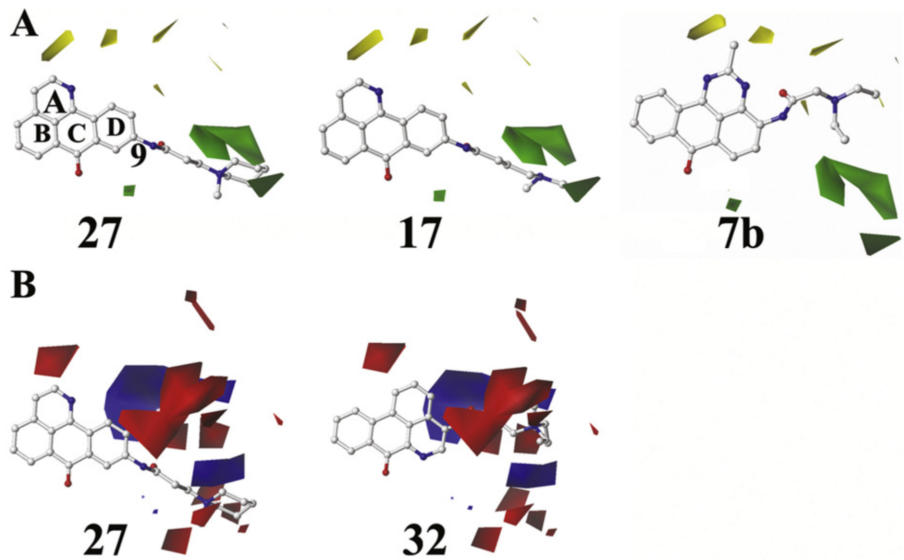

Fig. 3. (A) CoMFA steric STDEV*COEFF contour plots based on compounds **27**, **17**, and **7b**. Sterically favored areas are represented by green polyhedral, whereas sterically disfavorable are represented by yellow polyhedra. (B) CoMFA electrostatic STDEV*COEFF contour plots based on compounds **27** and **32**. Electropositively favored areas are represented by blue polyhedral, whereas electronegatively favored areas are represented by red polyhedra.

Fig. 3B displayed the electrostatic contour map of the CoMFA model. Blue and red regions represented electropositive favorable and electronegative favorable, respectively. There was a big blue region far away from the D ring, which indicated that electropositive substituents were favorable for inhibitory activity. This may be the reason why compounds with quaternary nitrogen were more active. For example, compounds **22**–**27** were more potent than compounds **13**–**18**, and **27** was the most potent compound among all derivatives. A red contour was found near A ring, indicating that the presence of nitrogen in this ring was necessary for inhibitory ability. This could explain why oxoisoaporphine derivatives were more potent AChE inhibitors than oxoaporphine derivatives. For example, compounds **28**–**34** gave lower AChE inhibitory activities than other oxoaporphine derivatives. Besides, though compounds **32**–**34** had quaternary nitrogen, they still gave lower activities. This implied that the nitrogen atom in A ring in oxoisoaporphine was important for activity. Other two red contours were found near D ring, suggesting that linker of substituent should be electron-rich.

4. Conclusion

In the present study, seven novel azaoxoisoaporphine derivatives were newly synthesized and their inhibitory activities toward AChE, BuChE, and Aβ aggregation were reported. Though they exhibited high inhibitory potency on Aβ aggregation, they gave no AChE or BuChE inhibition, which was very different from our previously reported oxoaporphine and oxoisoaporphine derivatives [3–5]. A reliable CoMFA model ($q^2 = 0.856$ and $r^2 = 0.986$) was based on their AChE inhibitory activities, and was further confirmed by the test-set validation ($q^2 = 0.873$, $r^2 = 0.937$, and slope $k = 0.902$) and Y-randomization tests. Based on this statistically significant and physically meaningful 3D-QSAR/CoMFA model, it was found that molecular shape, size, and charge played important roles in their inhibitory activities toward AChE among these derivatives. The generated contour maps also gave us more detail information about their relationship between the molecular structures and activities, which may help the rational molecular design of azaoxoisoaporphine, oxoaporphine, and oxoisoaporphine derivatives as anti-AChE and anti-AD agents.

Acknowledgements

We thank the Specialized Research Fund for the Doctoral Program of Higher Education (20110171110051), the Natural Science Foundation of China (21172272 and 21103234), Fundamental Research Funds for the Central Universities (11ykzd05), Natural Science Foundation of Guangdong Province (S2011030003190), and the International S&T Cooperation Program of China (2010DFA34630) for financial support of this study.

Appendix A. Supplementary data

Supplementary data associated with this article can be found, in the online version, at http://dx.doi.org/10.1016/j.jmgm.2013.02.003.

References

[1] Y. Rook, K.U. Schmidtke, F. Gaube, D. Schepmann, B. Wunsch, J. Heilmann, J. Lehmann, T. Winckler, Bivalent beta-carbolines as potential multitarget anti-Alzheimer agents, Journal of Medicinal Chemistry 53 (2010) 3611–3617.
[2] L. Mucke, Neuroscience: Alzheimer's disease, Nature 461 (2009) 895–897.
[3] H. Tang, F.X. Ning, Y.B. Wei, S.L. Huang, Z.S. Huang, A.S. Chan, L.Q. Gu, Derivatives of oxoisoaporphine alkaloids: a novel class of selective acetylcholinesterase inhibitors, Bioorganic and Medicinal Chemistry Letters 17 (2007) 3765–3768.
[4] H. Tang, Y.B. Wei, C. Zhang, F.X. Ning, W. Qiao, S.L. Huang, L. Ma, Z.S. Huang, L.Q. Gu, Synthesis, biological evaluation and molecular modeling of oxoisoaporphine and oxoaporphine derivatives as new dual inhibitors of acetylcholinesterase/butyrylcholinesterase, European Journal of Medical Chemistry 44 (2009) 2523–2532.
[5] Y.P. Li, F.X. Ning, M.B. Yang, Y.C. Li, M.H. Nie, T.M. Ou, J.H. Tan, S.L. Huang, D. Li, L.Q. Gu, Z.S. Huang, Syntheses and characterization of novel oxoisoaporphine derivatives as dual inhibitors for cholinesterases and amyloid beta aggregation, European Journal of Medical Chemistry 46 (2011) 1572–1581.
[6] B.W. Yu, L.H. Meng, J.Y. Chen, T.X. Zhou, K.F. Cheng, J. Ding, G.W. Qin, Cytotoxic oxoisoaporphine alkaloids from *Menispermum dauricum*, Journal of Natural Products 64 (2001) 968–970.
[7] V. Castro-Castillo, M. Rebolledo-Fuentes, C. Theoduloz, B.K. Cassels, Synthesis of lakshminine and antiproliferative testing of related oxoisoaporphines, Journal of Natural Products 11 (2010) 1951–1953.
[8] B. Chen, C. Feng, B.G. Li, G.L. Zhang, Two new alkaloids from *Miliusa cuneata*, Natural Product Research 6 (2003) 397–402.
[9] J. Ma, S.H. Jones, R. Marshall, R.K. Johnson, S.M. Hecht, A DNA-damaging oxoaporphine alkaloid from *Piper caninum*, Journal of Natural Products 7 (2004) 1162–1164.
[10] R.D. Cramer 3rd, D.E. Patterson, J.D. Bunce, Comparative molecular field analysis (CoMFA). 1. Effect of shape on binding of steroids to carrier proteins, Journal of the American Chemical Society 110 (1988) 5959–5967.

[11] R.D. Cramer 3rd, D.E. Patterson, J.D. Bunce, Recent advances in comparative molecular field analysis (CoMFA), Progress in Clinical and Biological Research 291 (1989) 161–165.
[12] X. Bu, L.W. Deady, G.J. Finlay, B.C. Baguley, W.A. Denny, Synthesis cytotoxic activity of 7-oxo-7H-dibenz[f,ij]isoquinoline and 7-oxo-7H-benzo[e]perimidine derivatives, Journal of Medicinal Chemistry 12 (2001) 2004–2014.
[13] F.X. Ning, X. Weng, Z.S. Huang, L.J. Gu, S.L. Huang, L.Q. Gu, A facile and efficient method for hydroxylation of azabenzanthrone compounds, Chinese Chemical Letters 22 (2011) 41–44.
[14] M.C. Clark, R.D. 3rd Cramer, N.V. Opden Bosch, Validation of the general purpose Tripos 5.2 force field, Journal of Computational Chemistry 10 (1989) 982–1012.
[15] J. Gasteiger, M. Marsili, Iterative partial equalization of orbital electronegativity—a rapid access to atomic charges, Tetrahedron 36 (1980) 3219–3228.
[16] S. Wold, A. Rhue, H. Wold, W.J.I. Dunn, The collinearity problem in linear regression. The partial least squares (PLS) approach to generalized inverses, SIAM Journal on Scientific Computing 5 (1984) 735–743.
[17] M. Clark, R.D. 3rd Cramer, The probability of chance correlation using partial least squares (PLS), Quantitative Structure–Activity Relationships 12 (1993) 137–145.
[18] B.L. Bush, R.B. Nachbar, Sample-distance partial least squares: PLS optimized for many variables, with application to CoMFA, Journal of Computer-Aided Molecular Design 7 (1993) 587–619.
[19] S. Wold, Cross-validatory estimation of the number of components in factor and principal components models, Technometrics 20 (1978) 397–405.
[20] V.D. Mouchlis, G. Melagraki, T. Mavromoustakos, G. Kollias, A. Afantitis, Molecular modeling on pyrimidine-urea inhibitors of TNF-α production: an integrated approach using a combination of molecular docking, classification techniques, and 3D-QSAR CoMSIA, Journal of Chemical Information and Modeling 52 (2012) 711–723.
[21] A. Golbraikh, A. Tropsha, Beware of q^2!, Journal of Molecular Graphics and Modelling 20 (2002) 269–276.
[22] G. Melagraki, A. Afantitis, H. Sarimveis, P.A. Koutentis, G. Kollias, O. Igglessi-Markopoulou, Predictive QSAR workflow for the in silico identification and screening of novel HDAC inhibitors, Molecular Diversity 13 (2009) 301–311.
[23] X.H. Zheng, Y.X. Shao, Z. Li, M. Liu, X. Bu, H.-B. Luo, X. Hu, Quantitative structure–retention relationship of curcumin and its analogues, Journal of Separation Science 35 (2012) 505–512.